

Asymmetric Excitation of Symmetric Single-mode Y-Junctions: The Radiation Mode Effects

Diaa A. M. Khalil, *Student Member, IEEE*, Pierre Benech and Smail Tedjini, *Member, IEEE*

Abstract—The asymmetric excitation of a symmetric single-mode Y-junction is studied in this work using two techniques: the standard BPM and a modal analysis based on the radiation spectrum. We found that the power splitting between the two outputs of the junction is strongly dependent on the coherent coupling of the odd radiation modes excited at the input of the junction. A GaAs/GaAlAs single mode junction excited by a single mode fiber is experimentally tested and a splitting ratio as high as 12 dB is obtained. Such a result, which could not be explained if the radiation field is neglected, proposes new applications of the Y-junction like an optical displacement sensor with a high sensitivity in the order of 5 dB/ μ m.

I. INTRODUCTION

BRANCHING elements and Y-junctions are important components currently used in integrated optics. These elements are usually required to be single-mode and the analysis of their performances depends mainly on the behavior of the fundamental guided mode. However, recent works have shown that the coherent coupling of radiation modes, generated in the junction, may be very efficient for loss reduction either for the junction itself [1], [2] or for a device based on it as the Mach-Zehnder interferometer [3]. In all these works the junction is assumed to be excited by its fundamental mode. This might be a good approximation if the input guide of the junction is long enough to filter, spatially, all the higher order radiation modes. In practical systems this is rarely satisfied as the size reduction is an important requirement. A complete study that takes into account the coherent coupling of the radiation modes in the branching elements is thus greatly required.

In this work we study the effects of the radiation mode coherent coupling on the performances of a symmetric single-mode Y-junction under the asymmetric excitation. The junction is excited by a single-mode optical fiber and the asymmetric excitation is due to fiber displacement. A classical analysis that considers only the guided mode propagation in the junction, gives a symmetric power division between the two branches whatever the fiber displacement and predicts only a reduction in the power coupled to the input waveguide. However, when the propagation of the radiation modes is taken into account, one output may be favoured with respect to the other due

to the coherent coupling of the odd radiation modes. This results in a distinction between the two symmetric outputs depending only on the excitation conditions. We use the standard BPM [4] as a non-modal analysis as well as a modal technique based on the spectrum of the radiation modes [2], [5] to analyze the performance of the junction. Our theoretical analysis shows that the power may be divided between the two outputs of the junction with a splitting ratio as high as 14 dB depending on the fiber displacement. The theoretical results were confirmed practically by testing two Y-junctions fabricated on GaAs strip loaded waveguide. This high splitting ratio, which could not be neglected, shows the importance of this study and opens the door for some new applications of the single-mode Y-junction. An example of these applications, proposed here, is its use as a displacement sensor where a sensitivity in the order of 5 dB/ μ m with a dynamic range of about 5 μ m is measured and a higher sensitivity may be obtained after optimizing the junction.

II. LOSSES OF THE Y-JUNCTION

The schematic diagram of the studied junction with the feeding fiber is shown in Fig. 1(a). The geometry of the junction is given in Fig. 1(b) where L_1 is the length of the input waveguide, L_2 is the length of the branching section, L_3 is the length of the two-arm section and W is the separation between the inner sides of the two output guides. The guiding structure is a GaAs/GaAlAs strip-loaded one whose cross-section is shown in Fig. 1(c). Using the effective index technique [6], the two dimensional waveguide could be replaced by a one dimension waveguide with an equivalent refractive index $n_{eq} = 3.392$, an equivalent step index $\delta n = 2.4 * 10^{-3}$ and a width $d = 5 \mu$ m; where the GaAs reflective index n_o is assumed to be 3.4 and the Al concentration in the two confinement layers is 3%. The optical guides are designed to be single mode at $\lambda = 1.3 \mu$ m and the geometry of the junction is chosen such that its losses become negligible (about 0.4 dB) when it is excited by the fundamental mode of its input guide. When the junction is excited by an optical field different from this mode, the losses are usually calculated as the sum of two terms:

- the injection losses due to the modal mismatching between the exciting field and the guided mode of the input guide of the junction
- the radiation losses of the junction itself.

This may be a good approximation when the input guide

Manuscript received July 10, 1992; revised July 30, 1992.

The authors are with LEMO, URA-CNRS 833, 23 Avenue des Martyrs, BP 257, 38016, Grenoble, Cedex, France.

IEEE Log Number 9203682.

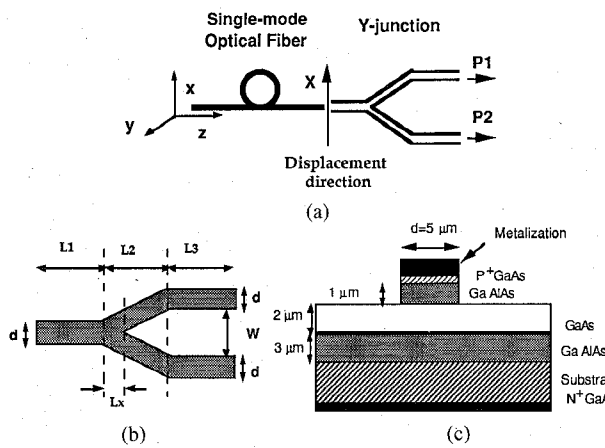


Fig. 1. Schematic diagram of the studied Y-junction: (a) System of excitation. (b) Geometry of the Y-junction. (c) Cross-section of guiding structure.

of the junction is so long that it filters all the radiation modes generated at the excitation. However, when the length L_1 is relatively small (with respect to the coherence length of the generated radiation modes [7]), the radiation modes may be coherently coupled to the output of the junction. This coupling becomes more important when the excitation of the junction is asymmetric. To underline this effect we calculate the losses of the junction shown in Fig. 1 under asymmetric excitation. The junction is excited using a single mode optical fiber. In our analysis, the fiber field is assumed to have a Gaussian distribution with a mode diameter D_f measured at $1/e^2$ of the maximum intensity. The excitation asymmetry is due to the displacement X_p of the fiber axis with respect to the junction axis of symmetry. Our input field is, thus written as

$$E_{in}(x) = E_o e^{-[2(X - X_p)/D_f]^2}. \quad (1)$$

The losses are calculated by two ways:

a) Considering only the injection losses, the input field is projected on the guided mode distribution of the input waveguide. The losses are then defined as

$$\text{Eta} = -10 \log_{10} \left[\frac{\left| \int_{-\infty}^{+\infty} E_{in}(x) \phi_{gm}^*(x) dx \right|^2}{\int_{-\infty}^{+\infty} |E_{in}(x)|^2 dx \int_{-\infty}^{+\infty} |\phi_{gm}(x)|^2 dx} \right] \quad (2)$$

where $\phi_{gm}(x)$ is the electric field distribution of the guided mode of the input guide.

b) Considering the coherent coupling of the radiation modes, the field distribution at the output of the junction is calculated using the BPM and then this field is projected on the output guided mode of the junction (Pmm in Fig. 2)

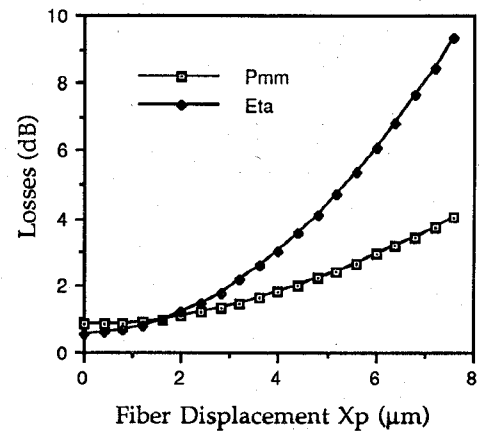


Fig. 2. Losses of the Y-junction calculated by two ways: Projecting the input Gaussian field on the guided mode (Eta). Calculating the output field by the BPM and projecting it on the output guided modes of the Y-junction (Pmm).

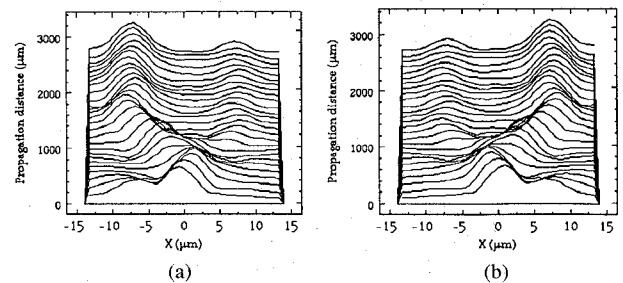


Fig. 3. Electric field distribution in the Y-junction under two asymmetric excitation conditions. (a) $X_p = -3$ μm. (b) $X_p = 3$ μm.

where $E_{o/p}(x)$ is the output field of the junction calculated by the BPM and the summation is performed on the two output guided modes of the junction. The BPM calculations are performed with an axial discretization $\Delta z = 5$ μm and a calculation window of 120 μm. The obtained results are shown in Fig. 2 for a junction with $L_1 = 440$ μm, $L_2 = 900$ μm, and $W = 10$ μm. The increasing difference between the two curves in Fig. 2 with X_p shows the importance of the radiation mode coherent coupling at asymmetric excitation. Moreover, the calculation of the optical field at the output of the junction shows that not only the junction losses are to be corrected but also its basic function, i.e., the power division. Fig. 3(a) and (b) show the optical field distributions in the junction, obtained by the BPM for $X_p = \pm 3$ μm. These results show that, while the junction is completely symmetric, the splitting ratio between the two outputs, $\eta = [P_1/P_2]$, may be different from unity depending on the excitation conditions. Actually, for X_p different from zero, a fraction of the input power is coupled to the odd radiation modes of the input waveguide. The interference of this group of modes with the even guided mode results in a field oscil-

$$\text{Pmm} = -10 \log_{10} \left[\sum_{1,2} \frac{\left| \int_{-\infty}^{+\infty} E_{o/p}(x) \phi_{gm_i}^*(x) dx \right|^2}{\int_{-\infty}^{+\infty} |E_{o/p}(x)|^2 dx \int_{-\infty}^{+\infty} |\phi_{gm_i}(x)|^2 dx} \right]$$

lation about the centre of the input guide. Thus, depending on the direction of the fiber displacement, the length of the input waveguide and the geometry of the junction, the power coupling to one branch may be favoured with respect to the other. To understand this behavior of the optical field we analyze the excitation of the input waveguide in more detail in the next section.

III. EXCITATION OF THE INPUT WAVEGUIDE

Fig. 4 shows the optical field distribution in a single-mode waveguide excited by a single-mode fiber for two excitation conditions. For $X_p = 0.0$ the fiber is perfectly aligned with the guide and then, only the even (guided and radiation) modes are excited in the guide. The existence of the even radiation modes results in spatial wings appearing in Fig. 4(a) at the initial propagation steps. For $X_p = 3 \mu\text{m}$ both the even and odd radiation modes are excited in the guide and the existence of the odd modes results in the field oscillations seen in Fig. 4(b). However, we remark that while the effect of the even radiation modes has disappeared rapidly in Fig. 4(a), the effect of the odd radiation modes persists in the waveguide for a long distance in Fig. 4(b). This is due to the spectral form of each group of modes generated at the exciting discontinuity. To obtain such a spectral form we decompose the input Gaussian field on the eigenmodes of the waveguide using the radiation spectrum technique previously presented by the authors [2], [5]. Thus, considering the TE field, where the extension for the TM field is quite similar, the electric field at any point, $E(x, z)$, could be written in the form [8]:

$$E(x, z) = \sum_i a_i \phi_i(x, \rho_i) \text{EXP}[-j\beta_i z] + \sum_q \int_0^{k_n} A_q(\rho) \phi_q(x, \rho) \text{EXP}[-j\beta z] d\rho \quad (4)$$

where $\phi(x, \rho)$ represents the profile in the x -direction of a mode with a propagation constant β and a spatial frequency ρ defined as

$$\rho^2 = k_{\text{no}}^2 - \beta_i^2 \quad (5)$$

where $k_{\text{no}} = n_{\text{eq}} * k_o$ is the equivalent substrate propagation constant.

The first summation in (4) extends over the guided modes, while the integration is performed over the continuum of the radiation modes. The second summation is used to consider both the even ($q = e$) and odd ($q = o$) radiation modes. The complex amplitudes a_i and $A(\rho)$ are determined from the exciting input field using the orthogonality of the modes and the normalization conditions [8]. Knowing $A(\rho)$ the power spectral density $S(\rho)$ associated with a mode of a spatial frequency ρ could be calculated [5]. Using this technique, the radiation spectrum of the input field corresponding to $X_p = 3 \mu\text{m}$ is given in Fig. 5 for the even and odd modes at the wavelength $\lambda = 1.3 \mu\text{m}$. We notice that the power of the even radiation modes is distributed over a wider range of spectrum than that of

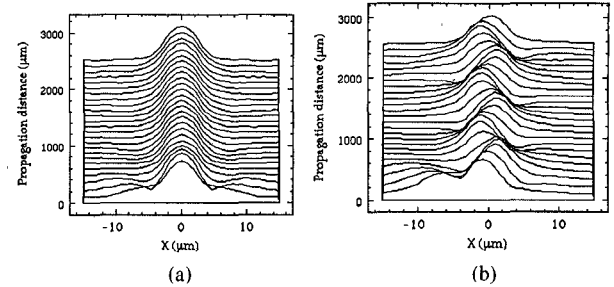


Fig. 4. Excitation of the input guide of the junction. (a) Symmetric excitation $X_p = 0.0$. (b) Asymmetric excitation $X_p = -3 \mu\text{m}$.

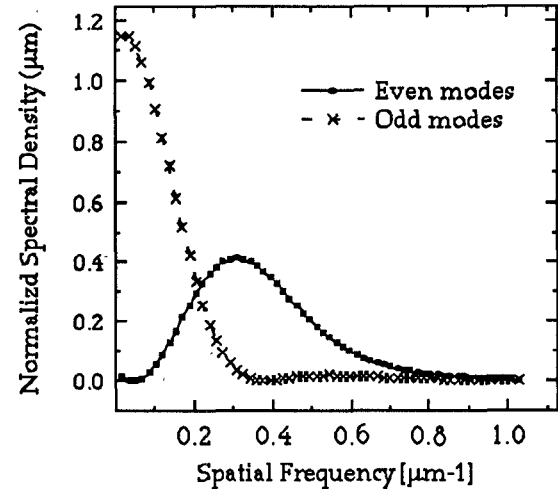


Fig. 5. Radiation spectrum of the even and odd radiation modes in the input guide.

the odd modes. This means that the group of odd radiation modes may propagate over a longer distance in the waveguide without phase distortion. Actually, we may define an effective propagation constant β_{eff} as well as a certain spectral width σ_β to be associated with each group of modes. For β_{eff} the value of the propagation constant of each mode could be weighted by its power spectral density to give:

$$\beta_{\text{eff}} = \int S(\rho) \beta d\rho / P_{\text{rm}} \quad (6)$$

where P_{rm} is the power of the concerned group of radiation modes defined by

$$P_{\text{rm}} = \int S(\rho) d\rho \quad (7)$$

The spectral width could be defined with respect to this effective propagation constant to be

$$\sigma_\beta^2 = \int S(\rho) (\beta - \beta_i)^2 d\rho / P_{\text{rm}} \quad (8)$$

Then, using these two parameters we may define two lengths, a beating length L_b at which the effective phase shift between the guided mode and the group of radiation modes is 2π , defined as

$$L_b = 2\pi / (\beta_{\text{gm}} - \beta_{\text{eff}}) \quad (9)$$

where β_{gm} is the propagation constant of the guided mode, and a coherence length L_c at which the phase shift between the radiation modes themselves becomes effectively π , defined as

$$L_c = \pi / \sigma_\beta. \quad (10)$$

Actually these parameters could be used to characterize the behavior of the radiation field in the waveguide. For the odd radiation modes the beating length gives approximately the periodicity of the field oscillations in the guide. For the even modes it should give the periodicity of the wings oscillation with respect to the field maximum; however these oscillations are not observed in Fig. 4 due to the rapid dispersion of the radiated field. On the other hand, the coherence length gives an indication to the distance at which the radiation mode interference with the guided mode is significant and then it characterizes the damping rate of the field oscillations. The relation between the coherence length and the damping rate of this interference depends mainly on the form of the radiation mode spectrum. For Gaussian spectral density distribution, this relation may be a direct one, similar to the case of the temporal coherence of laser sources. However, for non-Gaussian form, this relation is more complicated, especially when the spectrum is a non-symmetric one like that, shown in Fig. 5, for the odd radiation modes. For the spectrum shown in Fig. 5 we obtain:

$$L_b = 728.1 \mu\text{m} \text{ and } L_c = 1391.9 \mu\text{m}$$

for the odd radiation modes and

$$L_b = 492.1 \mu\text{m} \text{ and } L_c = 724.5 \mu\text{m}$$

for the even radiation modes.

and we have found that a propagation distance in the order of 4 to 5 times the coherence length is required for the damping of the odd radiation mode interference with the guided mode.

These parameters are functions of both the guiding properties (δn , λ , d etc) and the generating discontinuity. The spectrum shown in Fig. 5 is calculated for a guide of width $d = 5 \mu\text{m}$, $n_{eq} = 3.392$, and a step index $\delta n = 2.4 * 10^{-3}$ for a displacement X_p of $3 \mu\text{m}$ at the wavelength $\lambda = 1.3 \mu\text{m}$. In Fig. 6(a) and (b) we show their variations as a function of the fiber displacement X_p for the two wavelengths of interest $\lambda = 1.3 \mu\text{m}$ and $1.55 \mu\text{m}$. We remark that for smaller displacement the coherence length of the even radiation modes is shorter than that of the odd modes which explains the rapid dispersion of the field wings at symmetric excitation. Changing the wavelength from $1.3 \mu\text{m}$ to $1.55 \mu\text{m}$, the spectral parameters change slightly while the overall behavior of the curves remains the same. These parameters are of great importance for the junction design as they enable us to take into account the effect of the radiation mode coherent coupling by a simple model as will be seen in the next section.

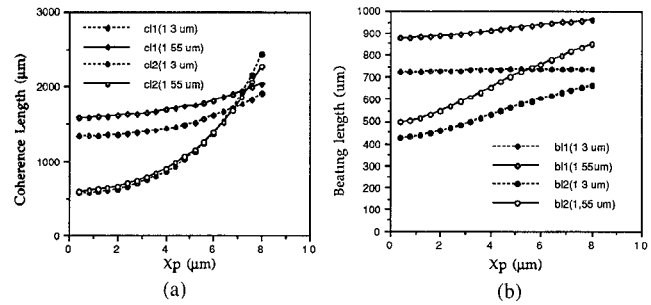


Fig. 6 Spectral parameters of the radiation modes excited at the input waveguide. For the odd modes $bl1$ and $cl1$ and for the even modes $bl2$ and $cl2$. (a) Coherence length. (b) Beating length.

IV. SPLITTING RATIO OF THE JUNCTION

One of the important parameters of the junction is its splitting ratio. As we have seen above, this splitting ratio may be a function of the excitation even when the junction is perfectly symmetric. For perfect alignment between the junction and the exciting fiber, the splitting ratio is always unity. However, with a slight fiber displacement, the splitting ratio may increase rapidly depending on the junction design as well as the operating wavelength. As seen above this splitting ratio results from the field oscillation in the input guide of the junction which favors the excitation of one junction arm with respect to the other. Thus, changing the length of the input guide L_1 is expected to modulate this ratio in an oscillatory way as it changes the position of the field maximum with respect to the output guides. Using the BPM we calculated the splitting ratio $\eta = P_1/P_2$ as a function of the length L_1 for the junction of Fig. 1 with $W = 10 \mu\text{m}$ and $L_2 = 900 \mu\text{m}$ and a fiber displacement $X_p = 3 \mu\text{m}$. For such a purpose the electric field distribution at the output of the junction is calculated and then projected on the guided modes of the two output guides. The ratio between the two projection coefficients is taken directly as the splitting ratio of the junction $\eta = P_1/P_2$.

The obtained results (Fig. 7) show the expected oscillatory behavior with a periodicity approximately equal to the beating length of the odd radiation modes calculated before. However, the damping rate of the oscillations seems to be less important than that estimated by the coherence length. This means that the calculated coherence length underestimates the effective length at which the effect of the odd radiation modes is significant. We believe that this is due to the non symmetry of the radiation spectrum of the odd modes with respect to its effective propagation constant. Actually this length becomes more significant when the spectrum approaches the Gaussian form (which is the case of the even modes). It is to be noted also that as L_1 tends to zero the splitting ratio becomes negative. This is due to the existence of a part of the field oscillations in the tapering section of the Y-junction. This means that the effective input guide length is longer than the physical length L_1 . The field oscillations in the tapering section is more complicated to

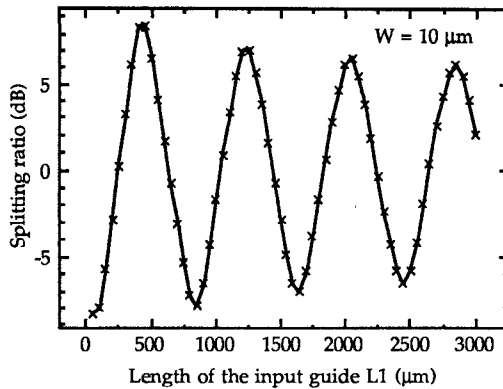


Fig. 7. Oscillatory behavior of the splitting ratio as a function of L_1 .

be analysed due to the axial variation of the effective propagation constants of the local guided and radiation modes. The axial variation would result in oscillations with a varying periodicity like that obtained usually in taper structures [9], [10]. In addition the increase of the guide width violates the single mode condition. The appearance of the odd guided modes absorbs the power of the odd radiation field and then the field oscillations result effectively from the interference between the two guided modes. While Fig. 7 is calculated for a certain fiber displacement $X_p = 3 \mu\text{m}$, the same conclusions could be obtained for other values of X_p .

Actually, increasing the fiber displacement X_p increases the amount of power coupled to the odd radiation modes and then the splitting ratio between the two outputs is expected to increase. However, the increase of X_p decreases also the power coupled to the guided mode. The variation of these powers is calculated in Fig. 8(a) as a function of the fiber displacement. One notices that, for a perfect alignment of the fiber, about 90% of the input power is coupled to the guided mode and no power is coupled to the odd radiation modes. For $X_p = 5 \mu\text{m}$ the power in the guided mode is approximately equal to that coupled to the odd radiation modes. As the field oscillations, responsible for the splitting ratio, result from the interference between the guided mode and the odd radiation modes, it is expected that the splitting ratio becomes maximum near $X_{pm} \approx 5 \mu\text{m}$. For X_p less than this value, the increase of X_p increases the oscillation amplitude and, consequently, the splitting ratio and vice-versa for X_p greater than X_{pm} . In the limiting case, when X_p becomes much greater than the guide width “ d ,” all the power is effectively coupled to the radiation modes and the optical field propagates in the equivalent substrate governed by the classical diffraction. This means that the splitting ratio takes the form of a symmetric S-curve with a maximum at X_{pm} . The value of X_{pm} depends mainly on both the guiding properties of the junction and the fiber mode diameter. These predictions are confirmed theoretically by calculating the splitting ratio as a function of the fiber displacement X_p using the BPM. The results obtained for an input

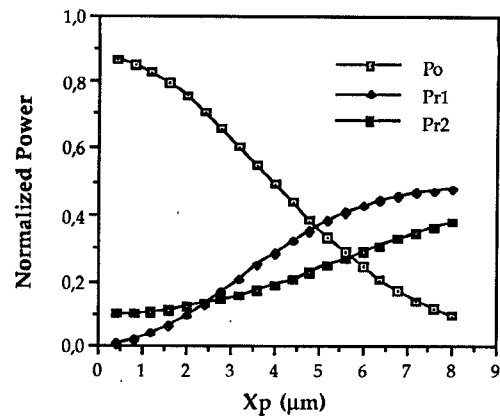


Fig. 8. Normalized Coupled Power for guided mode (P_o), odd radiation modes (P_{r1}), and even radiation modes (P_{r2}).

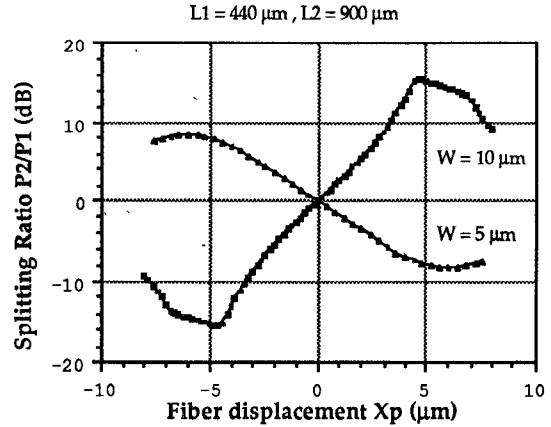


Fig. 9. Theoretical splitting ratio as a function of the fiber displacement ($L_1 = 440 \mu\text{m}$).

waveguide length $L_1 = 440 \mu\text{m}$, junction length $L_2 = 900 \mu\text{m}$ and two separations $W = 5$ and $10 \mu\text{m}$ are shown in Fig. 9. We obtain the expected S-curve with the maxima found approximately at the same fiber positions. However, two essential differences could be observed: the first is the inversion of curve with respect to the Y-axis, and the second is the reduction of the maximum value obtained for the splitting ratio. The inversion of the S-curve is, in fact, due to the reduction of the length of the tapering section in the Y-junction when changing W . Keeping $L_2 = 900 \mu\text{m}$ and changing W from 10 to $5 \mu\text{m}$ increases the length of the tapering section L_x (as shown in Fig. 1(b)) from $300 \mu\text{m}$ to $450 \mu\text{m}$. Moreover, the angle between the two junction arms is also reduced and then the coupling between them is increased. This results in an inversion of the field position with respect to the output guides as previously discussed. We observe also the change of the sensitivity $\sigma = \delta\eta / \delta X_p$ when changing the junction geometry while a good linearity (on a logarithmic scale) is obtained in the two cases. By measuring the ratio P_1/P_2 in dB, such a system may be used as an integrated optical displacement sensor with a high sensi-

tivity and a good linearity within an accepted dynamic range.

While the previous results are obtained for a wavelength $\lambda = 1.3 \mu\text{m}$, similar behavior is expected for other wavelengths. Changing the wavelength changes effectively the periodicity of the oscillations as it changes the beating length between the guided modes and the group of radiation modes as shown in Fig. 6. Thus depending on the required application, the length of the input guide L_1 may be chosen to minimize or to maximize the splitting ratio at the operating wavelength. For small lengths the variation of the wavelength does not affect greatly the splitting ratio. For long input guides the accumulation of the phase differences may lead to a significant effect which limits the spectral band of use. However, the increase of L_1 reduces also the coherence of the odd radiation modes and then their effect becomes less important.

V. EXPERIMENTAL RESULTS

To verify the previous theoretical predictions, the experimental set up shown in Fig. 10 is used. Two symmetric junctions are tested at the wavelength $\lambda = 1.3 \mu\text{m}$. The optical source used is a pigtailed D.F.B. single-mode laser diode. The two junctions have the same cross-sectional guiding structure shown in Fig. 1(b) with the geometrical dimensions $L_1 = 440 \mu\text{m}$, $L_2 = 900 \mu\text{m}$, $L_3 = 2700 \mu\text{m}$ and $W = 5$ and $10 \mu\text{m}$. To measure the field distribution at the output of the junction, a microscope objective of power 20 and a numerical aperture 0.27 is used to focus this field onto the lens of an infra-red camera connected to a monitoring unit and a P.C. for data acquisition. The fiber position is controlled using 3-dimensional piezoelectric cells. The junction is excited by a single mode optical fiber whose mode diameter D_f is found to be $12.5 \mu\text{m}$ at the operating wavelength $\lambda = 1.3 \mu\text{m}$. To measure the fiber mode diameter, the set-up shown in Fig. 10 is also used, without the Y-junction, and with a microscope objective of power 50 and a numerical aperture of 0.65. The optical intensity distribution at the output of the fiber is measured using the near field technique and then, curve-fitted by the Gaussian formula given in (1) with $X_p = 0$. Integrated optical directional couplers with different, well known, separations are used to calibrate the dimensions of the image obtained by the camera.

To determine the splitting ratio “ η ”, the optical intensity distribution at the output of the Y-junction is measured, for a given X_p and the ratio between the two maxima is calculated directly from the intensity distribution as

$$\eta = P1/P2 = [I_{1\max}/I_{2\max}]$$

where the two output guides are assumed to be identical. The advantage of the relative measurement is that it is independent of the absolute value of the power emitted from the laser source and then the laser stability is not a

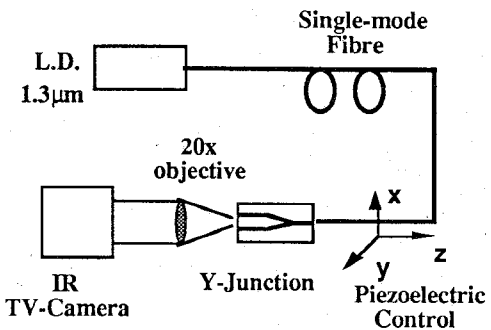


Fig. 10. Schematic diagram of the experimental set up used for measuring the splitting ratio.

critical parameter. However the effect of the background noise should be treated carefully. The relative response of the camera is calibrated using standard optical attenuators. Fig. 11(a) and (b) and c shows the optical intensity at the output of the junction of separation $W = 10 \mu\text{m}$, measured at $X_p = 0, \pm 1 \mu\text{m}$ respectively. The corresponding field distributions after data acquisition are also given. These field distributions are obtained within the linear range of the camera. However, for the corresponding photos, this was not respected as they are mainly presented for qualitative illustration. The relative displacement of the fiber is determined from the piezoelectric cell calibration, while its absolute position is referred to the axis of symmetry of the Y-junction. This reference is determined experimentally as the position at which the output of the junction is perfectly symmetric. The asymmetric intensity distribution is clearly observed in Fig. 11 for the displacements of $\pm 1 \mu\text{m}$. Repeating such a measurement for different values of X_p , the splitting ratio could be obtained as a function of the fiber displacement. The obtained results are shown in Fig. 12(a) and (b), for the two measured junctions. These results confirm well the theoretical predictions previously stated. For the first junction of $W = 10 \mu\text{m}$, a splitting ratio as high as 12 dB is obtained for about $2 \mu\text{m}$ displacement. This maximum value is reduced to about 4 dB in the case of the second junction with $W = 5 \mu\text{m}$. We remark also the inversion of the S-curve obtained in this case which confirms well the field oscillations in the input of the junction predicted theoretically.

The practical results show also a certain asymmetry with respect to X_p which is not predicted theoretically. This might be due to a certain uncontrolled asymmetry in the excitation that may result from either a non-perfect fiber cleaving or the existence of a little angle between the fiber and the Y-junction axes. Exciting the waveguide with a small tilt angle may also result in field oscillations that will perturb the measurements.

These experimental results show that the symmetric single-mode Y-junction could be used as a displacement sensor with a sensitivity in the order of $5 \text{ dB}/\mu\text{m}$ with a dynamic range in the order of $4 \mu\text{m}$. In addition to the

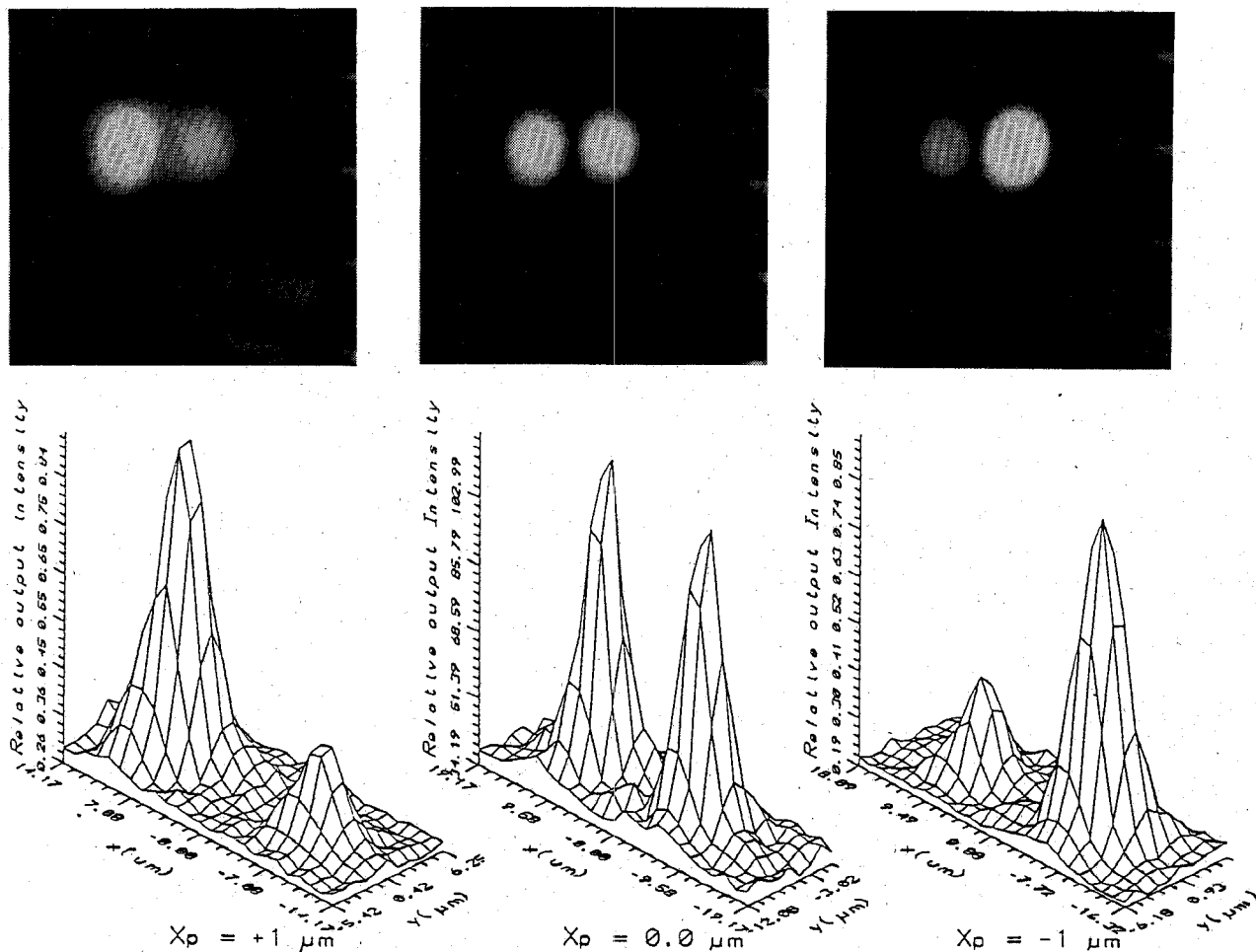


Fig. 11. Measured output intensity for three different positions of the fiber.

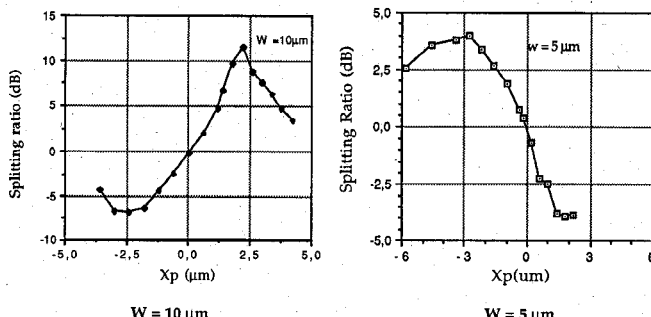


Fig. 12. Measured splitting ratio as a function of X_p for two junctions with $L_1 = 440 \mu\text{m}$, $L_2 = 900 \mu\text{m}$.

high sensitivity obtained, such a sensor is not sensitive to the laser source stability as it depends on a differential power measurement.

CONCLUSION

This work studies, for the first time, the performances of the symmetric single-mode Y-junction under asymmetric excitation. The theoretical analysis, based on the

non-modal BPM, shows that the asymmetric excitation may lead to a splitting ratio between the two outputs of the junction as high as 14 dB. These results are well explained when considering the radiation mode coherent coupling in the junction. A GaAs/GaAlAs Y-junction excited by a single mode optical fiber, has been tested. The obtained experimental results confirm well these theoretical predictions. Based on these results, the single-mode Y-junction may be used as a displacement sensor with a high sensitivity and good linearity. This effect may be also of great importance for other practical applications of the Y-junction like the Mach-Zehnder electrooptic intensity modulators in which this splitting ratio may reduce greatly its modulation depth.

REFERENCES

- [1] S. Chu and Pao-Lo Liu, "Low-loss coherent-coupling Y-branches," *Opt. Lett.*, vol. 16, no. 5, pp. 309-311, Mar. 1991.
- [2] D. Khalil and S. Tedjini, "Radiation modes in integrated optic discontinuities" Eleventh European symposium on optoelectronics, *Opto 91*, Paris, Mar. 26-28, 1991.
- [3] —, "Coherent coupling of radiation modes in Mach-Zehnder elec-

troptic modulators," *IEEE J. Quantum Electron.*, pp. 1236-1239, vol. 28, no. 5, May 1992.

[4] M. D. Feit, J. A. Fleck, "Light propagation in graded index optical fibers," *Applied Optics*, vol. 17, no. 24, pp. 3990-3998, Dec. 1978.

[5] —, "Coherent coupling of radiation modes in integrated optical structures," *IEEE-French Section/Cahier de la Recherche*, Accepted for publication.

[6] H. Kogelink, *Guided-Wave Optoelectronics*, Theodor Tamir, Ed., Berlin, Heidelberg: Springer verlag, 1988.

[7] H. F. Taylor, "Losses at corner bends in dielectric waveguides," *Applied Optics*, vol. 16, no. 3, pp. 711-716, Mar. 1977.

[8] D. Marcuse, *Light Transmission Optics*. New York: Van Nostrand Reinhold 1972.

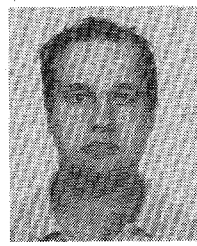
[9] I. Duport, P. Benech, D. Khalil, and R. Rimet, "Study of linear taper waveguides made by ion-exchange in glass," *J. of Physics-D: Applied Physics*, vol. 25, no. 6, pp. 913-918, June 14, 1992.

[10] B. Hermansson, D. Yevick, and P. Danielsen, "Propagating beam analysis of multimode waveguide tapers," *IEEE J. of Quantum Electron.*, vol. 19, no. 8, pp. 1246-1251, Aug. 1983.



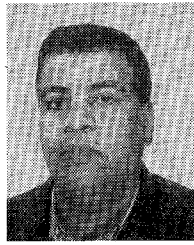
Diaa A. M. Khalil (S'91) was born in Cairo, Egypt in September 1961. He received the B.Sc. degree with honors and the M.Sc. degree, both in electrical engineering, from Ain-Shams University, Cairo, Egypt in 1984 and 1988, respectively. From 1984 to 1988 he was a Teaching Assistant at Ain-Shams University. While there, he was engaged in research in the linewidth of semiconductor lasers. From 1988 he joined the Laboratoire d'Electromagnétisme Microondes et Optoelectronique (LEMO) in Grenoble, France at which he is now working for his Ph.D degree in optoelectronics. His recent work is centered on the radiation mode effects in integrated optical structures.

Mr. Khalil is a student member of IEEE-Lasers and Electro-Optics Society, SPIE The International Society for Optical Engineering and the Topical Society of Laser Science in Egypt.



Pierre Benech was born in 1964, Dakar (Senegal). He received the diploma of Electrical Engineering, with honors, from the Ecole Nationale Supérieure d'Ingénieur Electricien de Grenoble, France, in 1987 and the Ph.D. degree in optoelectronics from the Institut National Polytechnic de Grenoble, France, in 1990. Since then he is assistant professor at the Ecole Nationale Supérieure d'Electronique et de Radioélectricité de Grenoble. He teaches electronics and guidedwave optics.

His main activity research concerns the optical fiber sensors, fiber devices, and passive integrated optics at the Laboratoire d'Electromagnétisme Microondes et Optoelectronique (LEMO) in Grenoble, France.



Smail Tedjini (M'91) was born in Behima (Algeria) on August 1956. He received the Matrice EEA degree from Joseph FOURIER University and the "Doctorat d'Etat Es-Sciences" from INPG (Grenoble, France) in 1980 and 1985, respectively.

In 1981 he joined the Laboratoire d'Electromagnétisme Microondes et Optoelectronique (LEMO) in Grenoble. From 1982 to 1986 he was involved in research on Microwave and Millimeterwave Integrated Circuits and specially the Fin-line technology. Since 1987 he is working on microwave modulation of optical signal. From 1990 he is the head of the Optomicroonde group in the LEMO and his research concerns the optical control of microwave signal and components as well as high speed integrated optoelectronic devices.

Dr. Tedjini is a member of the IEEE-Microwave Theory and Techniques Society, SPIE The International Society for Optical Engineering and the French SEE.